



HAL
open science

Upgrading Toughness and Glass Transition Temperature of Polydicyclopentadiene Upon Addition of Styrene-Ethylene-Butylene-Styrene Thermoplastic Elastomer

Quentin Beuguel, Evgueni Kirillov, Jean-Francois Carpentier, Sophie M. Guillaume

► To cite this version:

Quentin Beuguel, Evgueni Kirillov, Jean-Francois Carpentier, Sophie M. Guillaume. Upgrading Toughness and Glass Transition Temperature of Polydicyclopentadiene Upon Addition of Styrene-Ethylene-Butylene-Styrene Thermoplastic Elastomer. ACS Applied Polymer Materials, 2022, 4 (4), pp.2251-2255. 10.1021/acsapm.1c01803 . hal-03638772

HAL Id: hal-03638772

<https://hal.science/hal-03638772v1>

Submitted on 12 Apr 2022

HAL is a multi-disciplinary open access archive for the deposit and dissemination of scientific research documents, whether they are published or not. The documents may come from teaching and research institutions in France or abroad, or from public or private research centers.

L'archive ouverte pluridisciplinaire **HAL**, est destinée au dépôt et à la diffusion de documents scientifiques de niveau recherche, publiés ou non, émanant des établissements d'enseignement et de recherche français ou étrangers, des laboratoires publics ou privés.

Upgrading Toughness and Glass Transition Temperature of Polydicyclopentadiene Upon Addition of Styrene-Ethylene-Butylene-Styrene Thermoplastic Elastomer

Quentin Beuguel,^a Evgueni Kirillov (ORCID : 0000-0002-5067-480X),^a Jean-François Carpentier (ORCID: 0000-0002-9160-7662),^a Sophie. M. Guillaume (ORCID: 0000-0003-2917-8657)^{a,*}

^a Univ Rennes, CNRS, ISCR (Institut des Sciences Chimiques de Rennes) – UMR 6226, F-35000 Rennes, France

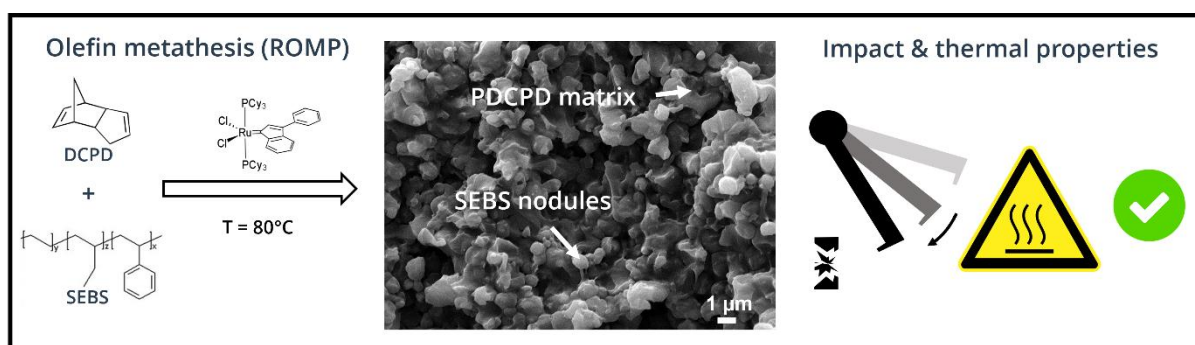
* Corresponding author: sophie.guillaume@univ-rennes1.fr

Abstract

Polydicyclopentadiene (PDCPD) thermoset, as commonly prepared by ring-opening metathesis polymerization (ROMP), features excellent mechanical, thermal and anti-corrosion properties, but lacks ductility and toughness. In situ addition of 2 to 8 wt% of Styrene-Ethylene-Butylene-Styrene (SEBS) thermoplastic during material preparation slightly alters the stiffness while improving its toughness and ductility. Remarkably, 4wt% SEBS increases PDCPD glass transition temperature T_g up to 165 °C (i.e. + 7 °C). Calorimetric analyses suggest that addition of SEBS, acting as a plasticizer during molding, reduces the polymerization time of DCPD. This result offers a simple method to adjust PDCPD impact properties and to increase its T_g .

Keywords: Polydicyclopentadiene (PDCPD), Styrene-Ethylene-Butylene-Styrene (SEBS), Ring-Opening Metathesis Polymerization (ROMP), thermoplastic elastomer (TPE), mechanical and thermal properties

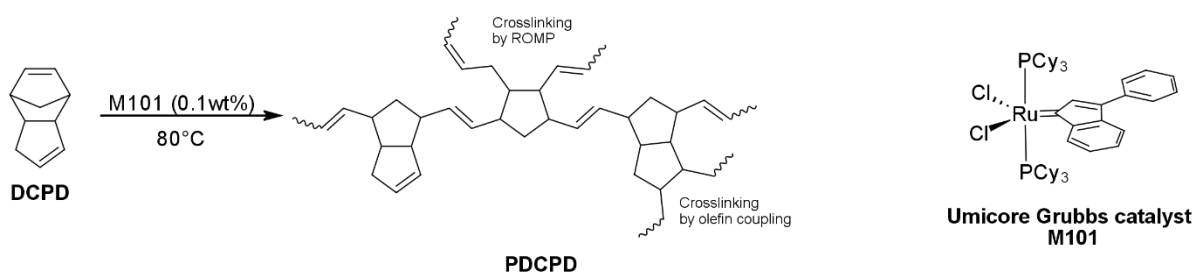
Graphical abstract



Since the elucidation of the ring-opening metathesis polymerization (ROMP) mechanism by Hérisson and Chauvin in 1971,¹ olefin metathesis catalysis for cycloolefin polymerization has been considerably developed.²⁻⁵ Among the variety of materials thus prepared, polydicyclopentadiene (PDCPD) has appeared as one of the most interesting thermosets,⁶ thanks to its high chemical and corrosion resistance, stiffness, and heat resistance for automotive, pipeline and building applications.^{7,8} Investigation of the polymerization mechanism of dicyclopentadiene (DCPD) revealed that the higher ring-strained norbornene first opens, resulting in the formation of a linear structure, followed by opening of the cyclopentene ring, ultimately resulting in a crosslinked network.⁹ Also, in the presence of ruthenium catalysts, PDCPD mainly crosslinks through metathesis but olefin addition reactions may also contribute to the crosslinking process, as reported by Davidson *et al.*^{10,11} In addition, much effort has been devoted to control the polymerization kinetics of DCPD in reaction injection molding process,^{12,13} leading to a highly crosslinked polymer with high thermal resistance, characterized by a glass transition temperature T_g close to 160 °C. Due to the absence of non-covalent interactions (e.g. hydrogen bonding) in the PDCPD network and to its propensity to form nanoscale voids, PDCPD has revealed remarkable impact performances much better than those of epoxy-based resins.^{14,15} However, the quasi-static mechanical properties of PDCD and the lack of ductility, are very far from those reported for crosslinked elastomers, for example in terms of elongation at break. This is yet a drawback for many applications such as body panels or field joint coating. The use of comonomers (e.g. cyclooctadiene, alkyl-norbornenes)¹⁶⁻¹⁸ or elastomers (e.g. polybutadiene,¹⁹ ethylene-propylene-diene (EPDM) monomer (< 5wt% ²⁰), forming copolymers with possibly pendant chains within the PDCPD network, has been proposed to improve these properties. However, in general, this drastically deteriorates the stiffness of PDCPD and decreases its T_g . In industry, blending of two polymers with different properties is a common approach to

improve the final properties of materials.²¹ Hence, the addition of non-miscible soft elastomers in a highly crosslinked epoxy has been shown to improve the ductility and toughness of the material, but it detrimentally decreases T_g .^{22–28} While addition of elastomers into PDCPD is reported to improve its flexibility and impact strength,²⁹ such an “in situ effect” on PDCPD network formation and T_g , directly correlated to its maximum service temperature, has to our knowledge never been reported.

The objective of the work reported herein is to highlight the role of a thermoplastic elastomer (TPE), namely Styrene-Ethylene-Butylene-Styrene (SEBS; Kraton™ G1652 commercial grade), a fully hydrogenated poly[styrene-*b*-(ethylene-*co*-butylene)-*b*-styrene] (Figure S1) strong and flexible TPE with excellent heat and UV resistance commonly used as impact modifier for engineering thermoplastics,³⁰ as an in situ component in the ruthenium-catalyzed ROMP of DCPD (Scheme 1). Also, the influence of SEBS on the final thermomechanical properties of PDCPD, especially its T_g and polymerization degree, is investigated.



Scheme 1. ROMP of DCPD

SEBS ($\phi_{\text{SEBS}} = 0\text{--}8$ wt%) was solubilized in DCPD for 48 h and then PDCPD/SEBS samples were prepared at 80 °C for 2 min using 0.1wt% M101 catalyst (in toluene), relative to the DCPD/SEBS mass. The main tensile (a), impact strength (b), thermomechanical (c) and calorimetric (d) properties of neat PDCPD and PDCPD/SEBS systems as a function of SEBS content (ϕ_{SEBS} , wt%) are summarized **Figure 1**. The corresponding tensile, impact, DMA and

DSC data were also determined (**Figures S2–S4, Table S1**). The addition of SEBS during ROMP and eventually into the resulting PDCPD decreases the stiffness of the material, as reported for epoxy/elastomer systems.^{22–28} In fact, the Young's modulus (E) decreases from 2.1 to 1.5 ± 0.1 GPa and maximum tensile stress (σ_{max}) declines from 50 to 34 ± 1 MPa (**Figure 1a**). On the other hand, the impact strength and elongation at break (ϵ_{max}) reach a maximum of 34 ± 3 kJ·m⁻² and 15 ± 3 %, respectively, for $\phi_{SEBS} = 4\text{wt}\%$ (**Figures 1a,1b**). This trend agrees with the improved toughness and ductility of the material upon addition of an elastomer in a thermoset, in particular in terms of enhanced cavitation, shear banding or crack pinning phenomena, and reduced stiffness. However, as commonly reported, the material's stiffness is reduced at the same time.^{22–28} For our present PDCPD/SEBS systems, whitening of samples is observed during tensile test (**Figure S2b**), and a rough surface is observed by SEM after impact (**Figure 2c**), as compared to the smooth surface observed for neat PDCPD (**Figures 2a,2b**). These observations suggest a cavitation mechanism and other adsorption mechanisms limiting crack propagation, due to the presence of micrometric nodules in PDCPD (**Figures 2c,2d**), as commonly observed for thermoset/thermoplastic blends.³¹ A maximum ductility and toughness values at $\phi_{SEBS} = 4\text{wt}\%$ (**Figures 1a,1b**) are also hinting at a larger elastomer concentration leading to particle agglomeration that decreases the yielding area density and/or favors failure defects and failure growth.^{23,25–28}

Rewardingly, in the present PDCPD/SEBS materials, these classical variations of mechanical properties are coupled with an unexpected improvement of the thermal properties. Indeed, the glass transition is observed over a narrower temperature range (**Figure S3**) and reaches a maximum value of $T_g = \text{ca. } 165 \pm 1$ °C (**Figure 1c**) at $\phi_{SEBS} = 4\text{wt}\%$ (as compared to $T_g \sim 158 \pm 1$ °C for neat PDCPD). Moreover, the rubbery plateau, E'_r , as determined by DMA, increases from ca. 10 to 19 ± 1 MPa, corresponding to a molar mass between crosslinks, M_c , varying from 1 200 to 600 g·mol⁻¹. These observations are in contrast with

those previously reported for other highly crosslinked thermosets such as epoxy materials where the addition of a soft elastomer or plasticizer tends to decrease the T_g .^{22,24–27} In addition, the polymerization degree of DCPD, α , as measured by DSC (Figure S4), increases from $75 \pm 5 \%$ for neat PDCPD to $87 \pm 5 \%$ for PDCPD/SEBS with $\phi_{SEBS} = 4\text{wt}\%$ (Figure 1d). In summary, the best compromise between mechanical and thermal properties is obtained for $\phi_{SEBS} = 4\text{wt}\%$ in PDCPD (Figure 1).

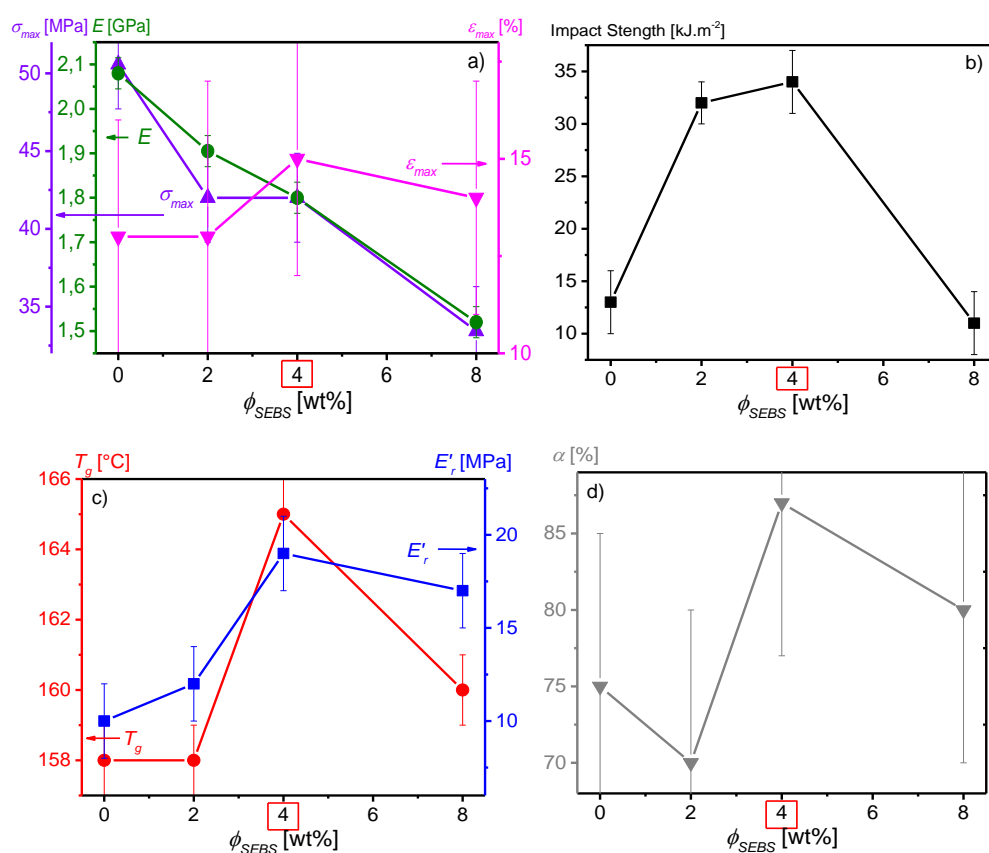


Figure 1. Main tensile (a), impact (b), thermomechanical (c) and calorimetric (d) characteristics of neat PDCPD and PDCPD/SEBS as a function of SEBS content, ϕ_{SEBS}

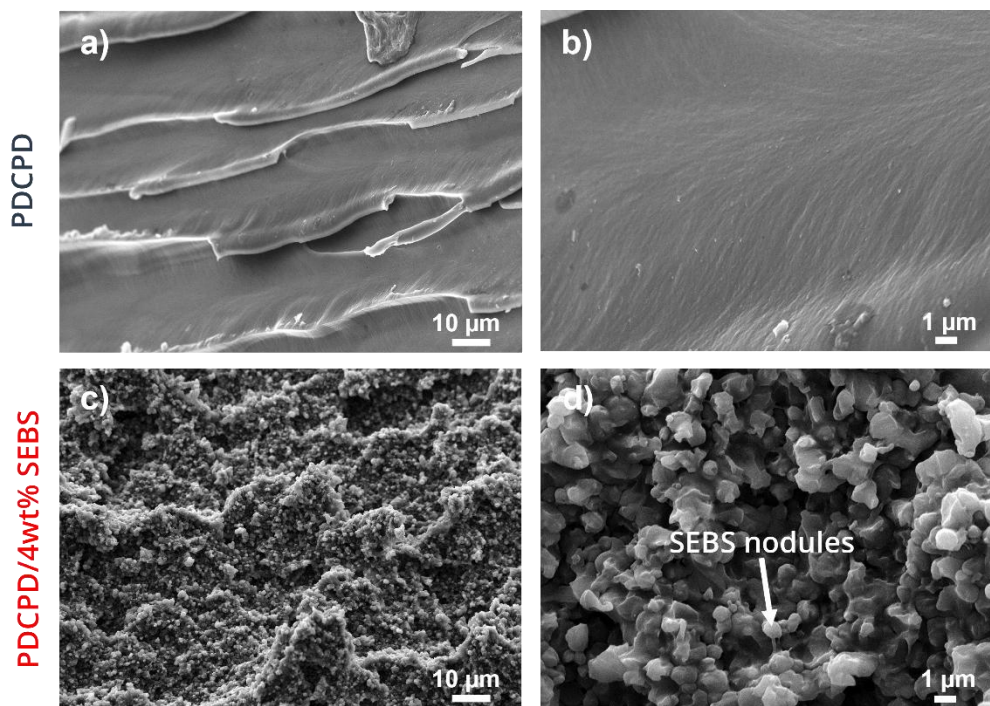


Figure 2. SEM images of neat PDCPD (a and b) and PDCPD/4wt% SEBS material (c and d)

In order to elucidate this unexpected yet valuable effect of SEBS on the thermal properties of PDCPD, in situ temperature measurements (**Figure 3**), isothermal DSC (for 5 min at various temperatures) and further complementary anisothermal analyses (following isotherms; from -40 to 300 °C at 30 °C·min $^{-1}$) were performed, and the polymerization kinetics at each isothermal temperature (**Figure 4**) was studied for both neat DCPD and DCPD/4wt% SEBS.

As shown in **Figure 3**, similar maximum in situ temperatures $T_{max} = \text{ca. } 180$ °C and 130 °C were recorded for both DCPD and DCPD/4wt% SEBS systems, respectively, in the core or at the mold wall of the plate. This is due to the very exothermic polymerization reaction associated with the energy released by cyclic olefin ring opening.³² A slight reaction delay (ca. 5 s) was observed at $\phi_{\text{SEBS}} = 4\text{wt}\%$, probably due to the resin viscosity (η , measured using a Brookfield viscosimeter) increasing from 6 to 96 cP and/or to the DCPD dilution effect. High in situ temperatures (> 100 °C) were measured in the mold for few tens of seconds (**Figure 3**).

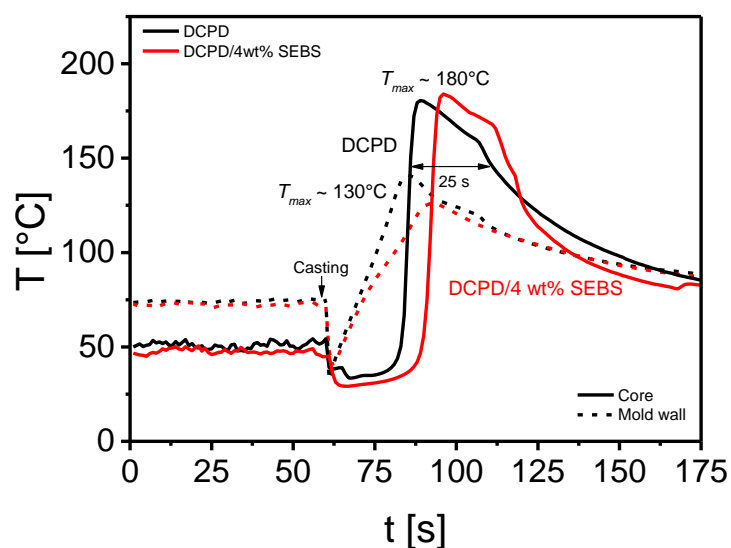


Figure 3. In situ temperature monitoring over time during molding of neat DCPD and DCPD/4wt% SEBS

The polymerization degree, α , and polymerization time to reach 95% of the maximum polymerization degree at each isothermal temperature, $t_{0.95}$, monitored as a function of isothermal temperature, T_{iso} , are plotted **Figure 4**. After 5 min isotherm, the DCDP conversion is maximal at each temperature. Classically, α increases following an exponential law (Arrhenius model) as a function of isothermal temperature, for both systems. However, the $t_{0.95}$ value significantly decreases with $\phi_{SEBS} = 4$ wt%. More precisely, in the latter conditions, this polymerization time is 5–30 s shorter than that for neat DCPD (depending on T_{iso}) (**Figure 4**). This is within the same order of magnitude as the time measured during molding, at high temperature (**Figure 3**). We thus suggest that macromolecules of SEBS, thanks to their solubility in DCPD, act as a lubricant or plasticizer. This phenomenon induces the mobility of the polymer material during polymerization, thus enabling in turn a higher DCPD polymerization rate. This would account for improving polymerization degree of DCPD at short molding time, thus increasing the crosslinking density and the glass transition temperature of PDCPD in the presence of SEBS.

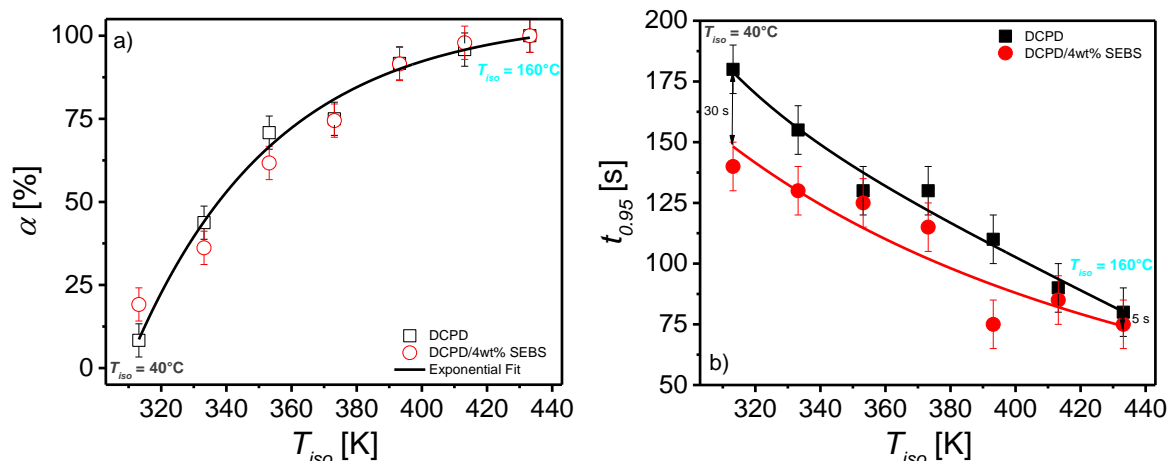


Figure 4. Polymerization degree, α , (a) and time variations to reach 95% of the maximum polymerization degree at each isothermal temperature, $t_{0.95}$, (b) as a function of isothermal temperature, T_{iso} .

In summary, we have demonstrated that the addition of a small amount (4wt%) of SEBS TPE significantly increases both the toughness and T_g of PDCPD (in direct correlation to its maximum application temperature) without dramatically affecting its stiffness. These thermomechanical properties improvements are suggested to arise from the plasticizing effect of SEBS during molding, leading to better polymerization degree and crosslinking density of PDCPD, as supported by DSC and DMA analyses. This unexpected result paves the way to the tuning of PDCPD properties upon adjusting the elastomer chemical structure and morphology. Further studies changing the elastomer nature are currently in progress for maximizing toughening effect and T_g value.

Supporting Information

Experimental section. ^1H NMR spectrum of SEBS commercial grade used. Raw thermo-mechanical data of PDCPD/SEBS samples (tensile tests, Izod impact, DMA & DSC analysis).

Acknowledgements

The authors thank the French Foundation of La Maison de la Chimie for its financial support. We are grateful to Mr. Francis Gouttefangeas (UAR 2025 ScanMAT, Rennes, France) for SEM images.

References

- (1) Hérisson, P. J.-L.; Chauvin, Y. Catalyse de Transformation Des Oléfines Par Les Complexes Du Tungstène. II. Télomérisation Des Oléfines Cycliques En Présence d'oléfines Acycliques. *Die Makromol. Chemie* **1971**, *141* (1), 161–176. <https://doi.org/10.1002/MACP.1971.021410112>.
- (2) Grubbs, R. H.; Tumas, W. Polymer Synthesis and Organotransition Metal Chemistry. *Science*. **1989**, *243* (4893), 907–915. <https://doi.org/10.1126/science.2645643>.
- (3) Buchmeiser, M. R. Homogeneous Metathesis Polymerization by Well-Defined Group VI and Group VIII Transition-Metal Alkylidenes: Fundamentals and Applications in the Preparation of Advanced Materials. *Chem. Rev.* **2000**, *100* (4), 1565–1604. <https://doi.org/10.1021/cr990248a>.
- (4) Sutthasupa, S.; Shiotsuki, M.; Sanda, F. Recent Advances in Ring-Opening Metathesis Polymerization, and Application to Synthesis of Functional Materials. *Polym. J.* **2010**, *42* (12), 905–915. <https://doi.org/10.1038/pj.2010.94>.
- (5) Abera Tsedalu, A. A Review on Olefin Metathesis Reactions as a Green Method for the Synthesis of Organic Compounds. *J. Chem.* **2021**, *2021*, 1–14. <https://doi.org/10.1155/2021/3590613>.
- (6) Kovačič, S.; Slugovc, C. Ring-Opening Metathesis Polymerisation Derived Poly(Dicyclopentadiene) Based Materials. *Mater. Chem. Front.* **2020**. <https://doi.org/10.1039/d0qm00296h>.
- (7) Magalhães Camboa Sá, A. Development of Lightweight and Cost-Efficient Exterior Body Panels for Electric Vehicles, PhD Thesis, Porto University (Portugal), 2016.
- (8) Global Polydicyclopentadiene (PDCPD) Market Size 2021 Industry Share, Business Strategies, Growth Analysis, Regional Demand, Revenue, Key Manufacturers and 2025 Forecast Research Report Says Industry Research Biz - MarketWatch / <https://www.marketwatch.com/press-release/global-polydicyclopentadiene-pdcpd-market-size-2021-industry-share-business-strategies-growth-analysis-regional-demand-revenue-key-manufacturers-and-2025-forecast-research-report-says-industry-research-biz-2021-10> (accessed Oct 26, 2021).
- (9) Fisher, R. A.; Grubbs, R. H. Ring-Opening Metathesis Polymerization of Exo-Dicyclopentadiene: Reversible Crosslinking by a Metathesis Catalyst. *Makromol. Chemie. Macromol. Symp.* **1992**, *63* (1), 271–277. <https://doi.org/10.1002/masy.19920630120>.
- (10) Davidson, T. A.; Wagener, K. B.; Priddy, D. B. Polymerization of Dicyclopentadiene: A Tale of Two Mechanisms. *Macromolecules* **1996**, *29* (2), 786–788. <https://doi.org/10.1021/ma950852x>;
- (11) Davidson, T. A.; Wagener, K. B., The Polymerization of Dicyclopentadiene: An Investigation of Mechanism. *J. Mol. Catal. A Chem.* **1998**, *133* (1–2), 67–74. [https://doi.org/10.1016/S1381-1169\(98\)00091-0](https://doi.org/10.1016/S1381-1169(98)00091-0).

- (12) Yao, Z.; Zhou, L.; Dai, B.; Cao, K. Ring-Opening Metathesis Copolymerization of Dicyclopentadiene and Cyclopentene through Reaction Injection Molding Process. *J. Appl. Polym. Sci.* **2012**, *125* (4), 2489–2493. <https://doi.org/10.1002/app.36359>.
- (13) Kim, H. G.; Son, H. J.; Lee, D. K.; Kim, D. W.; Park, H. J.; Cho, D. H. Optimization and Analysis of Reaction Injection Molding of Polydicyclopentadiene Using Response Surface Methodology. *Korean J. Chem. Eng.* **2017**, *34* (7), 2099–2109. <https://doi.org/10.1007/s11814-017-0102-5>.
- (14) Knorr, D. B.; Masser, K. A.; Elder, R. M.; Sirk, T. W.; Hindenlang, M. D.; Yu, J. H.; Richardson, A. D.; Boyd, S. E.; Spurgeon, W. A.; Lenhart, J. L. Overcoming the Structural versus Energy Dissipation Trade-off in Highly Crosslinked Polymer Networks: Ultrahigh Strain Rate Response in Polydicyclopentadiene. *Compos. Sci. Technol.* **2015**, *114*, 17–25. <https://doi.org/10.1016/j.compscitech.2015.03.021>.
- (15) Long, T. R.; Elder, R. M.; Bain, E. D.; Masser, K. A.; Sirk, T. W.; Yu, J. H.; Knorr, D. B.; Lenhart, J. L. Influence of Molecular Weight between Crosslinks on the Mechanical Properties of Polymers Formed: Via Ring-Opening Metathesis. *Soft Matter* **2018**, *14* (17), 3344–3360. <https://doi.org/10.1039/c7sm02407j>.
- (16) Yang, G.; Mauldin, T. C.; Lee, J. K. Cure Kinetics and Physical Properties of Poly(Dicyclopentadiene/5-Ethylidene-2-Norbornene) Initiated by Different Grubbs' Catalysts. *RSC Adv.* **2015**, *5* (73), 59120–59130. <https://doi.org/10.1039/C5RA05335H>.
- (17) Boggioni, L.; Galotto, N. G.; Bertini, F.; Tritto, I. Terpolymerization of Substituted Cycloolefin with Ethylene and Norbornene by Transition Metal Catalyst. *Polymers.* **2016**, *8*(3), 60. <https://doi.org/10.3390/polym8030060>.
- (18) Dean, L. M.; Wu, Q.; Alshangiti, O.; Moore, S.; Sottos, N. R. Rapid Synthesis of Elastomers and Thermosets with Tunable Thermomechanical Properties. *ACS Macro Lett.* **2020**. <https://doi.org/10.1021/acsmacrolett.0c00233>.
- (19) Yang, Y. S.; Lafontaine, E.; Mortaigne, B. Curing Study of Dicyclopentadiene Resin and Effect of Elastomer on Its Polymer Network. *Polymer.* **1997**, *38* (5), 1121–1130. [https://doi.org/10.1016/S0032-3861\(96\)00599-X](https://doi.org/10.1016/S0032-3861(96)00599-X).
- (20) German, D. Y. Physico-Mechanical Characteristics of the PDCPD-EPDM-30 Composites. In *Chemistry and chemical technology in the XXI century: materials of the XIX International Scientific and Practical Conference of Students and Young Scientists named after Professor LP Kulev*; 2018; pp 484–485.
- (21) Utracki, L. A. *Commercial Polymer Blends*; Springer, 1998.
- (22) Yee, A. F.; Pearson, R. A. Toughening Mechanisms in Elastomer-Modified Epoxies. *J. Mater. Sci. 1986 217* **1986**, *21* (7), 2462–2474. <https://doi.org/10.1007/BF01114293>.
- (23) Liu, S. H.; Nauman, E. B. Effect of Cross-Linking Density on the Toughening Mechanisms of Rubber-Modified Thermosets. *J. Mater. Sci. 1991 2624* **1991**, *26* (24), 6581–6590.

<https://doi.org/10.1007/BF00553681>.

- (24) Liu, J.; Sue, H. J.; Thompson, Z. J.; Bates, F. S.; Dettloff, M.; Jacob, G.; Verghese, N.; Pham, H. Nanocavitation in Self-Assembled Amphiphilic Block Copolymer-Modified Epoxy. *Macromolecules* **2008**, *41* (20), 7616–7624. <https://doi.org/10.1021/ma801037q>.
- (25) Lu, J.; Wool, R. P. Additive Toughening Effects on New Bio-Based Thermosetting Resins from Plant Oils. *Compos. Sci. Technol.* **2008**, *3–4* (68), 1025–1033. <https://doi.org/10.1016/J.COMPSCITECH.2007.07.009>.
- (26) Thomas, R.; Yumei, D.; Yuelong, H.; Le, Y.; Moldenaers, P.; Weimin, Y.; Czigany, T.; Thomas, S. Miscibility, Morphology, Thermal, and Mechanical Properties of a DGEBA Based Epoxy Resin Toughened with a Liquid Rubber. *Polymer*. **2008**, *49* (1), 278–294. <https://doi.org/10.1016/j.polymer.2007.11.030>.
- (27) Bain, E. D.; Knorr, D. B.; Richardson, A. D.; Masser, K. A.; Yu, J.; Lenhart, J. L. Failure Processes Governing High-Rate Impact Resistance of Epoxy Resins Filled with Core–Shell Rubber Nanoparticles. *J. Mater. Sci.* **2016**, *51* (5), 2347–2370. <https://doi.org/10.1007/s10853-015-9544-5>.
- (28) Caldoná, E. B.; Leon, A. C. C. De; Pajarito, B. B.; Advincula, R. C. A Review on Rubber-Enhanced Polymeric Materials. *Polymer Reviews* **2016**, *57* (2), 311–338. <https://doi.org/10.1080/15583724.2016.1247102>.
- (29) Daniel W. Klosiewicz. US4657981A: Dicyclopentadiene Polymer Containing Elastomer, 1987.
- (30) Abreu, F. O. M. S.; Forte, M. M. C.; Liberman, S. A. SBS and SEBS Block Copolymers as Impact Modifiers for Polypropylene Compounds. *J. Appl. Polym. Sci.* **2005**, *95* (2), 254–263. <https://doi.org/10.1002/APP.21263>.
- (31) Folkes, M. J.; Hope, P. S. *Polymer Blends and Alloys*, London: Blackie Academic & Professional. **1993**.
- (32) Ivin, K. .; Mol, J. *Olefin Metathesis and Metathesis Polymerization*, Elsevier. **1997**.

SUPPORTING INFORMATION

Upgrading Toughness and the Glass Transition Temperature of Polydicyclopentadiene upon Addition of Styrene–Ethylene–Butylene–Styrene Thermoplastic Elastomer

Quentin Beuguel,^a Evgueni Kirillov (ORCID : 0000-0002-5067-480X),^a Jean-François Carpentier (ORCID: 0000-0002-9160-7662),^a Sophie. M. Guillaume (ORCID: 0000-0003-2917-8657)^{a,†}

^a Univ Rennes, CNRS, ISCR (Institut des Sciences Chimiques de Rennes) – UMR 6226, F-35000 Rennes, France

[†] Corresponding author E mail: sophie.guillaume@univ-rennes1.fr

Table of contents

Experimental section	S16
Figure S1. ¹ H NMR (300 MHz, CDCl ₃ , 25 °C) full (bottom) and zoomed (top) spectra of SEBS (Kraton™ G1652); * stands for residual solvent signal.	S17
Figure S2. Average tensile curves for neat PDCPD and PDCPD/SEBS samples (a) and photos of tensile specimens of neat PDCPD and PDCPD/4wt% SEBS during tensile test (b).....	S20
Table S1. Main mechanical properties of neat PDCPD and PDCPD/SEBS samples.....	S20
Figure S3. DMA analysis of neat PDCPD and PDCPD/SEBS samples	S21
Figure S4. Anisothermal DSC thermograms of neat DCPD and DCPD/SEBS resins and polymerized samples	S22
Figure S5. Quasi-isothermal (a, c) and associated anisothermal (b, d) DSC thermograms for neat DCPD (a, b) and DCPD/4wt% SEBS (c, d) samples. Normalized polymerization degrees, $\alpha(t)$, at various isothermal temperatures T_{iso} during isotherms (e – k)	S24

Experimental section

Materials and methods.

Liquid DCPD/TCPD mixture (85/15 *w/w* as determined by ^1H NMR) was prepared by heating solid DCPD (99% purity; Maruzen Petrochemical Co., Ltd., Ichihara, Japan) at 200°C for 4 h under argon at atmospheric pressure. This monomer mixture is referred to DCPD.

Styrene-Ethylene-Butylene-Styrene, a poly[styrene-*b*-(ethylene-*co*-butylene)-*b*-styrene] (SEBS; 30wt% styrene content; KratonTM G1652) TPE (physically crosslinked), was supplied by Kraton Corporation (Houston, USA; $T_g = -36\text{ }^\circ\text{C}$ and $96\text{ }^\circ\text{C}$, average number molar mass (M_n) ca. $54\ 000\ \text{g}\cdot\text{mol}^{-1}$).¹ No signals arising from potential residual double bonds derived from the butylene monomer (δ_{H} between 5 and 6 ppm)² within the main backbone of SEBS were detected by ^1H NMR spectroscopy (Figure S1) thus supporting its fully hydrogenated characteristics. First generation ruthenium catalyst (M101[®] Umicore (CAS number: 250220-36-1); Sigma-Aldrich, Saint-Louis, USA), dissolved (2wt%) in toluene (HPLC grade), was used for the DCPD ROMP. This catalyst was selected for its lower activity as compared to a second generation ruthenium catalyst, thereby avoiding a rapid gelation and enabling a more homogenous mixing before casting.

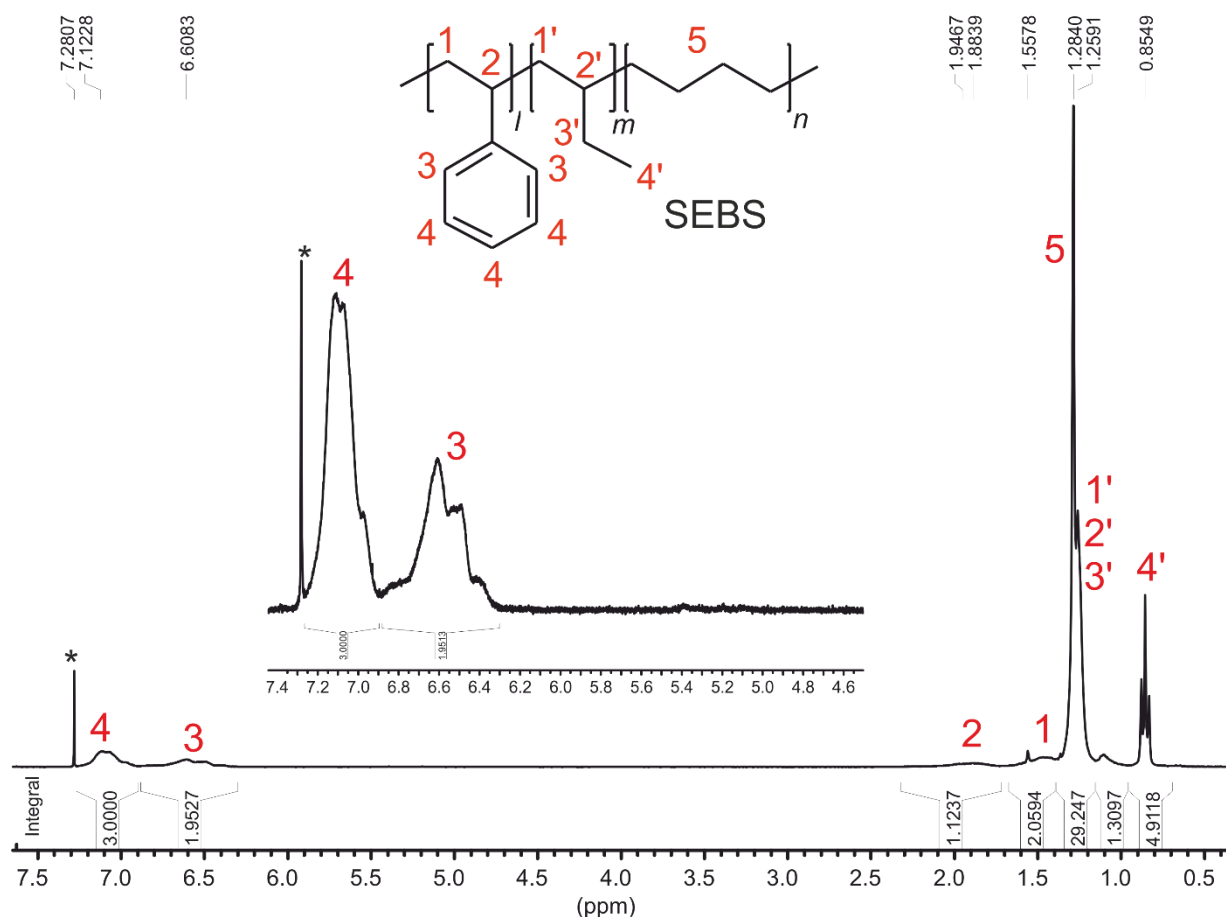


Figure S1. ¹H NMR (300 MHz, CDCl₃, 25 °C) full (bottom) and zoomed (top) spectra of SEBS (Kraton™ G1652); * stands for residual solvent signal.

Tensile tests were performed with a AGS-X50kN machine (Shimadzu) equipped with a force sensor of 50 kN, at a speed of 50 mm·s⁻¹ on 110 × 15 × 4 mm 1B-specimens (ISO 527-1 & -2).

Izod impact was performed on a IT 503 Pendulum Impact Tester (Tinius Olsen) on 2 mm- notched 80 × 10 × 4 mm specimens (ISO 180). The initial impactor height was fixed at 610 mm with an angle of 145° from the sample, equipped with a hammer with a radius of 335 mm and a mass of 463 g.

The mechanical tests were carried out at room temperature and the average and standard deviation values (used as error bars) were obtained from 5 independent measurements for each sample.

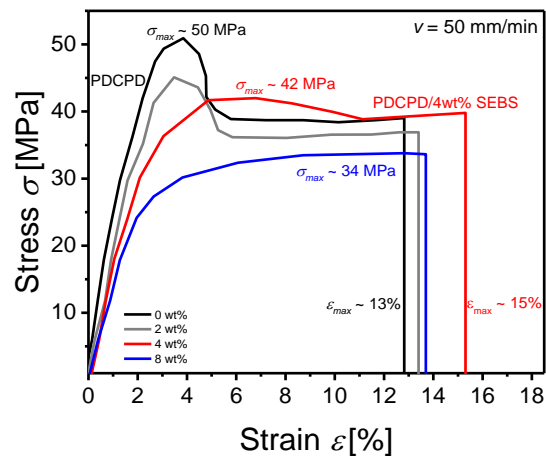
Micrometric images were recorded on Izod impact fractured samples at room temperature, with vacuum gold metalized surface, using a Scanning Electron Microscope (SEM) JEOL JSM 7100 F, operating at 10 kV.

The thermomechanical properties were measured on a DMA Q800 (TA Instruments) from 30 to 240 °C at 3°C·min⁻¹ and $f = 1$ Hz, in bending mode on 17.5 × 5 × 4 mm specimens. The glass transition temperature (T_g) determined at the maximum of the damping factor $\tan \delta$, and the elastic modulus at the rubbery state (E'_r) directly related to the molar mass between crosslinks by M_c ca. $3RT\rho/E'_r$ (where R , T and ρ are the universal gas constant, temperature and density, respectively), are reported with $\pm 1^\circ\text{C}$ and $\pm 1\text{MPa}$ precision, respectively.

Differential Scanning Calorimetry (DSC) anisotherms were performed on resins (ca.10 mg) using standard aluminum pans (with 0.1wt% of M101 catalyst in toluene) or plate, during the first heating from -40 °C to 300 °C at 30 °C·min⁻¹, under a continuous flow of helium (25 mL·min⁻¹), using a DSC-131 apparatus (Setaram) calibrated with indium. Quasi-isothermal analyses were carried out at $T_{iso} = 20$ to 160 °C for 5 min. The isothermal temperature (T_{iso}) was reached at 100 °C·min⁻¹ (maximum heating rate of the DSC) starting from -40 °C. The polymerization degree α ($\pm 5\%$) was calculated from the ratio between the residual reaction enthalpy (ΔH) of the solid sample and the total enthalpy of the resin. The time $t_{0.95}$ (± 10 s) was determined as the time necessary to reach 95% of the normalized maximum polymerization degree α for each isothermal temperature T_{iso} .

Typical preparation procedure. A weight fraction of SEBS ($\phi_{\text{SEBS}} = 0\text{--}8$ wt%) was solubilized in DCPD for 48 h at room temperature under magnetic stirring. Then, 0.1wt% M101 catalyst, relative to the DCPD/SEBS mass (in toluene) was incorporated in DCPD/SEBS (300 g) under magnetic stirring over a 5 s period. The mixture was next casted in a 300 × 200 × 4 mm aluminum mold at 80 °C, for 2 min.

Figure S2 presents the average tensile curves for neat PDCPD and PDCPD/SEBS samples. The corresponding main tensile and impact mechanical properties are reported in **Table S1**. Classically, the stiffness of the sample decreases, characterized by a drop of both the Young's modulus E and the maximum tensile stress σ_{max} , from 2.1 to 1.5 ± 1 GPa and from 50 to 34 ± 1 MPa, for neat PDCPD to PDCPD/8wt% SEBS, respectively. In parallel, the strain at break, ϵ_{max} , in tensile test slightly increases to $15 \pm 3\%$ (from $13 \pm 3\%$ for neat PDCPD) (**Figure S2.a**). This is correlated to an elongation mechanism change with the addition of SEBS, favoring cavitation as suggested by specimen whitening (**Figure S2.b**). More significantly, the Izod impact strength reaches 34 ± 3 kJ·m⁻² (from 13 ± 3 kJ·m⁻²), with 4 wt% of SEBS (**Table S1**). Both a maximum ductility and toughness value are noted for this SEBS concentration.



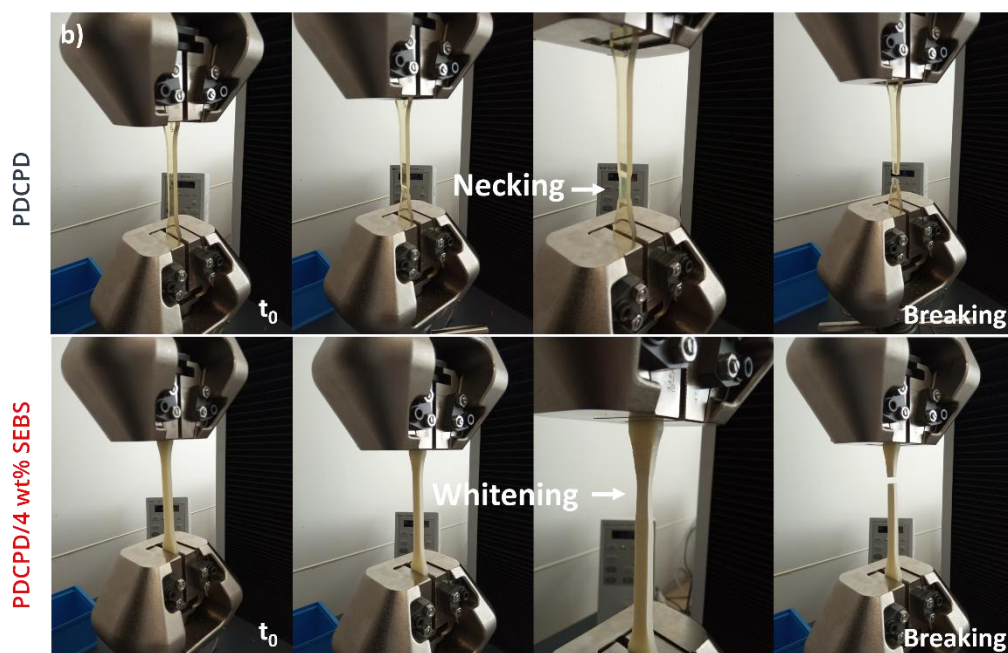


Figure S2. Average tensile curves for neat PDCPD and PDCPD/SEBS samples (a) and photos of tensile specimens of neat PDCPD and PDCPD/4wt% SEBS during tensile test (b)

Table S1. Main mechanical properties of neat PDCPD and PDCPD/SEBS samples

SEBS concentration [wt%]	Tensile test			Izod Impact
	Young's Modulus E [GPa]	Max stress σ_{max} [MPa]	Strain at break ϵ_{max} [%]	Impact strength [kJ.m ⁻²]
0	2.1 ± 0.1	50 ± 1	13 ± 3	13 ± 3
2	1.8 ± 0.1	45 ± 1	13 ± 4	32 ± 2
4	1.8 ± 0.1	42 ± 1	15 ± 3	34 ± 3
8	1.5 ± 0.1	34 ± 1	14 ± 5	11 ± 3

Figure S3 shows the variation of the storage modulus, E' , and the damping factor, $\tan \delta$, as a function of temperature for neat PDCPD and PDCPD/SEBS samples, as measured by DMA. The addition of SEBS increases the glass transition temperature (T_g) of PDCPD, the elastic rubbery modulus plateau (E'_r), and narrows the range of the glass transition temperature. Maximum values were measured for $\phi_{SEBS} = 4\text{wt\%}$, where T_g and E'_r reached 165 ± 1 °C and 19 ± 1 MPa, as compared to 158 ± 1 °C and 10 ± 1 MPa for neat PDCPD, respectively.

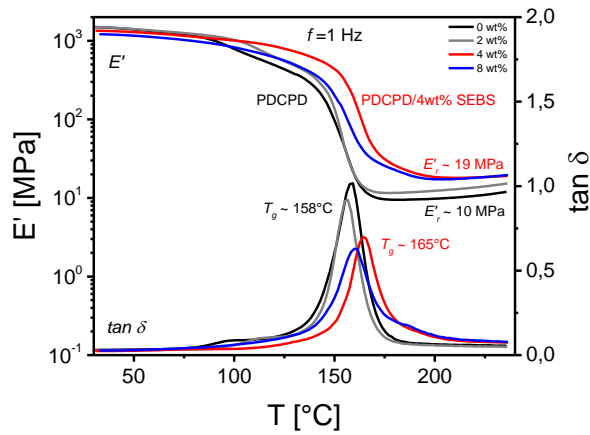


Figure S3. DMA analysis of neat PDCPD and PDCPD/SEBS samples

Figure S4 presents the anisothermal DSC thermograms (ramp from -40 to 300 °C at 30 °C·min $^{-1}$) of resin and molded samples for neat DCPD and DCPD/SEBS with ϕ_{SEBS} ranging from 2 to 8wt%. The total reaction enthalpy, ΔH , of the resin roughly decreases with the concentration of SEBS from 240 (for neat DCPD) to 225 J·g $^{-1}$ (for 8wt%), directly associated to the SEBS fraction in the material which does not react by ROMP. However, the polymerization degree, α , is maximal for the plate with $\phi_{\text{SEBS}} = 4\text{wt}\%$, where α ca. $1 - \frac{\Delta H_{\text{plate}}}{\Delta H_{\text{resin}}} = 1 - \frac{30}{235} = 0.87 = 87 \pm 5\%$, as compared to $75 \pm 5\%$ for neat PDCPD (**Figure S4**).

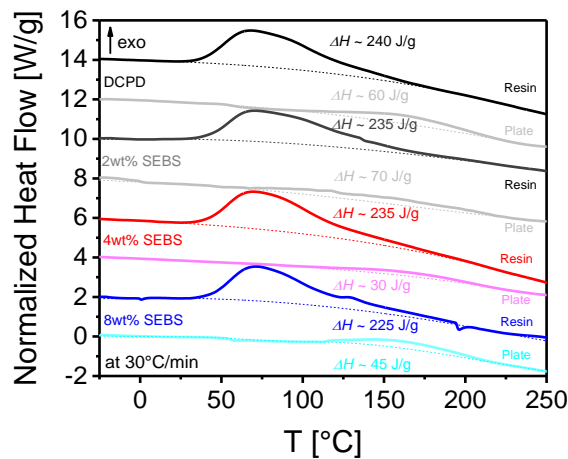
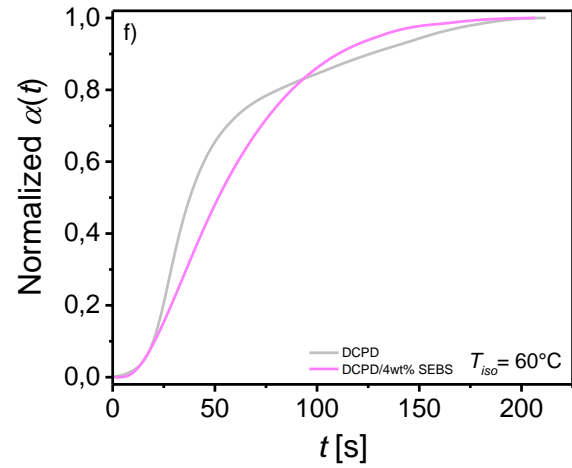
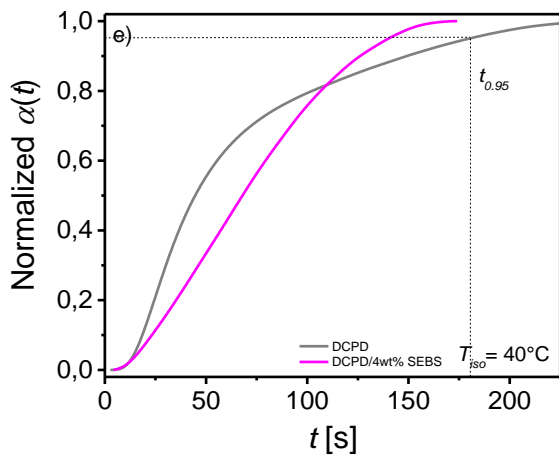
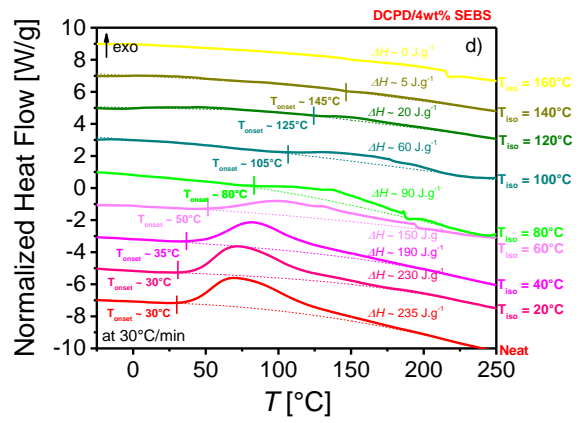
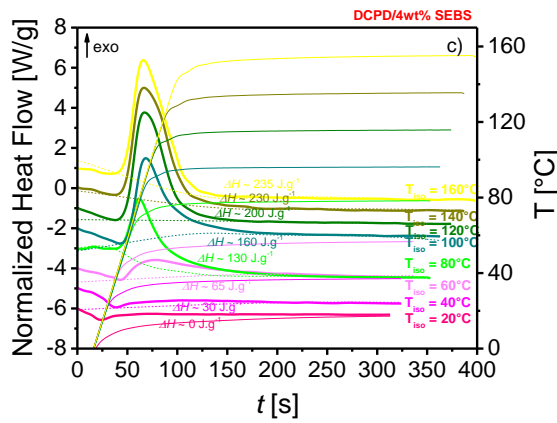
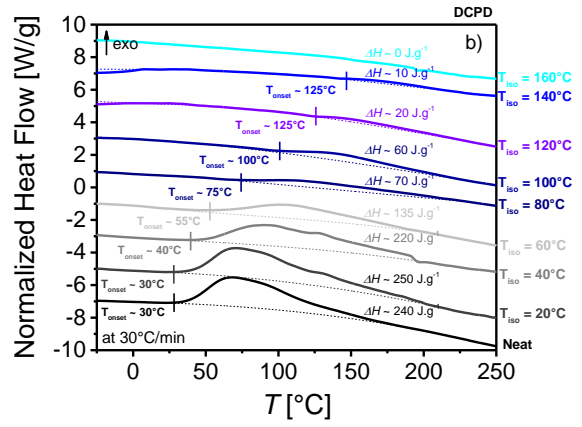
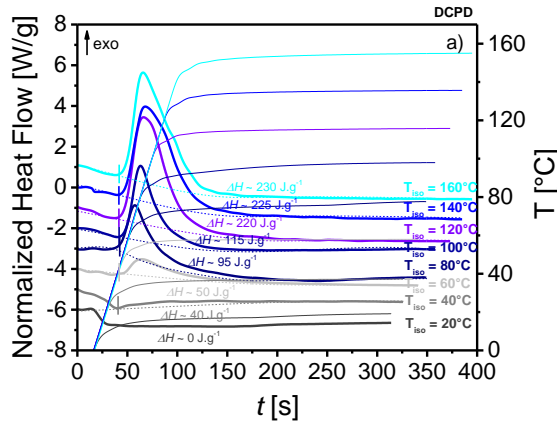


Figure S4. Anisothermal DSC thermograms of neat DCPD and DCPD/SEBS resins and polymerized samples

Figure S5 shows the quasi-isothermal (named as isothermal in the main manuscript for clarity) DSC thermograms (ramp from 0 °C to T_{iso} at $100\text{ °C}\cdot\text{min}^{-1}$ before 5 min isotherm at T_{iso}) (a, c) of samples at different temperatures from $T_{iso} = 20$ to 160 °C and their associated complementary anisothermal DSC thermograms (ramp from -40 °C to 300 °C at $30\text{ °C}\cdot\text{min}^{-1}$ after isotherms) (b, d), of neat DCPD (a, b) and DCPD/4 wt% SEBS (c, d). The normalized polymerization degrees $(0-1)$ $(f - 1)$ $\alpha(t)$, calculated from isothermal DSC thermograms and the enthalpy reaction measured at each T_{iso} , are plotted as a function of time, t , for neat DCPD and DCPD/4wt% SEBS. For all samples, the reaction enthalpy, ΔH , as measured for isothermal and anisothermal tests, are complementary and roughly equal to 240 (for neat DCPD, **Figures S5a and S5b**) and $235\text{ J}\cdot\text{g}^{-1}$ (for $\phi_{SEBS} = 4\text{wt}\%$, **Figures S5c and S5d**), in agreement with results reported in **Figure S4**. In more details, for all isothermal temperatures (**Figures S5e – k**), the polymerization rate appears to be delayed at the onset of the reaction in the presence of 4wt% of SEBS; this is likely due to the resin viscosity (as measured using a Brookfield viscosimeter) that increases from $\eta = 6$ to 96 cP and/or a DCPD dilution effect. However, systematically, the polymerization time required to reach 95% of the maximum normalized polymerization degree, $t_{0.95}$, is in the order of a few tens of seconds shorter, especially above $T_{iso} > 100\text{ °C}$ where the SEBS phase is completely plasticized. We suggest that the soft SEBS macromolecule plays the role of a lubricant or plasticizer during ROMP, thereby improving the polymerization rate of DCPD during the short molding time (few tens of seconds (**Figure 3**)), especially at high temperatures.



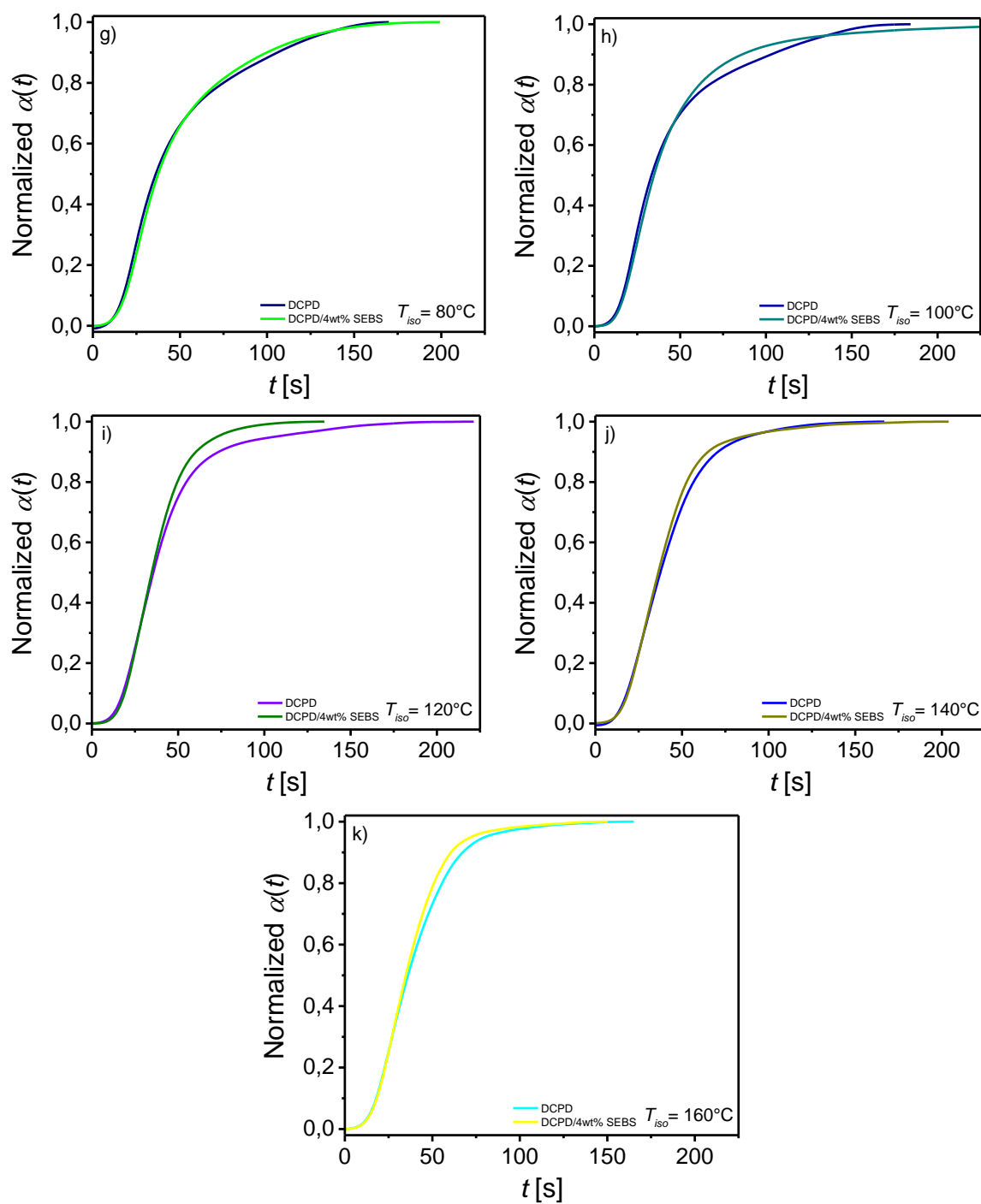


Figure S5. Quasi-isothermal (a, c) and associated anisothermal (b, d) DSC thermograms for neat DCPD (a, b) and DCPD/4wt% SEBS (c, d) samples. Normalized polymerization degrees, $\alpha(t)$, at various isothermal temperatures T_{iso} during isotherms (e – k)

References

- (1) Muller, D.; Garcia, M.; Salmoria, G. V.; Pires, A. T. N.; Paniago, R.; Barra, G. M. O. SEBS/PPy.DBSA Blends: Preparation and Evaluation of Electromechanical and Dynamic Mechanical Properties. *J. Appl. Polym. Sci.* **2011**, *120* (1), 351–359. <https://doi.org/10.1002/app.33141>.
- (2) Chiang, C.-H.; Tsai, J.-C. Hydrogenation of Polystyrene- b -Polybutadiene- b - Polystyrene Mediated by Group (IV) Metal Metallocene Complexes. *J. Polym. Sci. Part A Polym. Chem.* **2017**, *55* (13), 2141–2149. <https://doi.org/10.1002/pola.28589>.